COMPUTATIONAL RESEARCH PROGRESS IN APPLIED SCIENCE & ENGINEERING (CRPASE)

CRPASE: TRANSACTIONS OF CIVIL AND ENVIRONMENTAL ENGINEERING

Journal homepage: http://www.crpase.com

CRPASE: Transactions of Civil and Environmental Engineering 8 (2) Article ID: 2781, 1–9, June 2022 ISSN 2423-4591

Research Article

Modeling of Local Scour Depth Around Bridge Pier Using FLOW 3D

M. Sobhi Alasta [1*], Ahmed Shakir Ali Ali [2], Saman Ebrahimi [2], Muhammad Masood Ashiq [2], Abubaker Sami Dheyab [1], Adnan AlMasri [3], Anass Alqatanani [1], Mahdis Khorram [2]

[1] *Department of Civil Engineering, University of Gaziantep, 27410 Şehitkamil, Gaziantep, Turkey*
[2] *Department of Civil Engineering, University of Memphis, 3720 Alumni Ave, Memphis, TN 38152, USA*
[3] *Department of Civil and Environmental Engineering, German Jordanian University, Amman 11180, Jordan*

Keywords

Local Scour,
Flow-3D,
Bridge Pier,
Circular Pier.

Abstract

The most crucial issue that causes bridge failure is local scour, especially during flood events. Therefore, modeling scouring is an essential method to examine the possibility of bridge failure due to scour. Various numerical and laboratory models were conducted to investigate the scour depth around hydraulic structures. This paper investigates the performance of the CFD model to simulate the local scour depth around the bridge pier using Flow-3D. First, the model was built and then calibrated based on experimental outcomes. Further, the results show that the CFD model can provide a good agreement between the numerical and experimental models. The CFD model successfully imitates the scour depth, flow, and velocity around the bridge pier.

1. Introduction

Due to the population growth and civilization and their severe impacts on environmental issues, i.e., climate change, temperature, floods, water quality, and availability, have shown lots of attention among researchers [1-6]. As a result, the need to find the optimum design with the highest performance and capability and the lowest impact on the surrounding ambient feels more than past [7-13]. Scour can be mentioned as one of the side effects of artificial structures on the environment.

Scour is defined as the removal of material from the base and edges of the river and near the piers and abutments that consistently happens due to discharge acceleration and the erosive activity of flow [14-16]. Scour around bridge piers happens during overflow, commonly due to ripples [17, 18]. It is the leading cause of bridge collapse worldwide [19], with critical financial losses jeopardizing residents. Also, several bridges are parts of the vital infrastructure for supporting connectivity during natural catastrophes [20].

The mechanism of scouring around a circular cylinder was investigated broadly using various laborites in the literature [21, 22]. The mentioned research outcomes demonstrated that the scour is driven by the increased local shear stresses provoked by the acceleration of discharge close to the pier, as shown in Figure 1. Another reason is the existence of a powerful downflow force at the face of the bridge pier. The horseshoe vortex is initially tiny and vulnerable with a circular pier cross-section, but the dimensions and forces grow with the scour hole's expansion and downwards movement [23]. Pier and abutment damage due to scouring and deterioration of the base of the river were identified as being the fundamental cause of the bridge's failure [24]. The Federal Highway Administration

* Corresponding Author: M. Sobhi Alasta
E-mail address: Sobhialasta@gmail.com

Received: 07 April 2022; Revised: 28 April 2022; Accepted: 13 May 2022

https://doi.org/10.52547/crpase.8.2.2781

Academic Editor: **Vahid Najafi Moghadam Gilani**

Please cite this article as: M. Sobhi Alasta, A. Ali Ali, S. Ebrahimi, M. Masood Ashiq, A. Sami Dheyab, A. Al Masri, A. Alqatanani, M. Khorram, Modeling of Local Scour Depth Around Bridge Pier Using FLOW 3D, Computational Research Progress in Applied Science & Engineering, CRPASE: Transactions of Civil and Environmental Engineering 8 (2022) 1–9, Article ID: 2781.

has revealed that 60% of bridges fail in the USA because of scouring [25], and about 60 bridges collapse per year in the United States [26]. Also, investigations indicated that failure data from various nations assembled shows that the natural hazards are the highest reason behind the bridge collapsing [27], as shown in Figure 1.

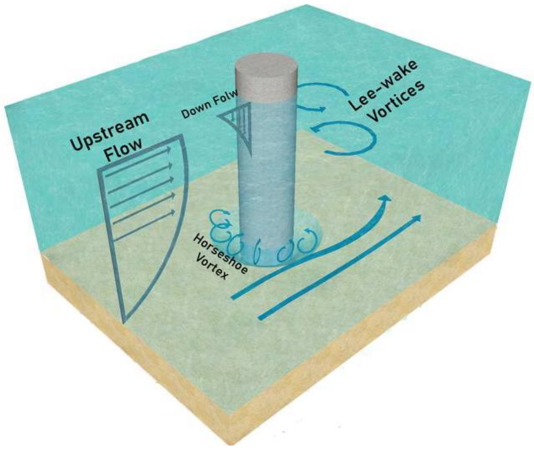

Figure 1. Mechanism of Scour

[28] showed that 500 collapsed bridges in the USA during 1989 -2000 were because of scouring. Therefore, investigating decrement in the riverbed due to scour is essential for developing transportation infrastructure and bridge piers' dimensions and shape.

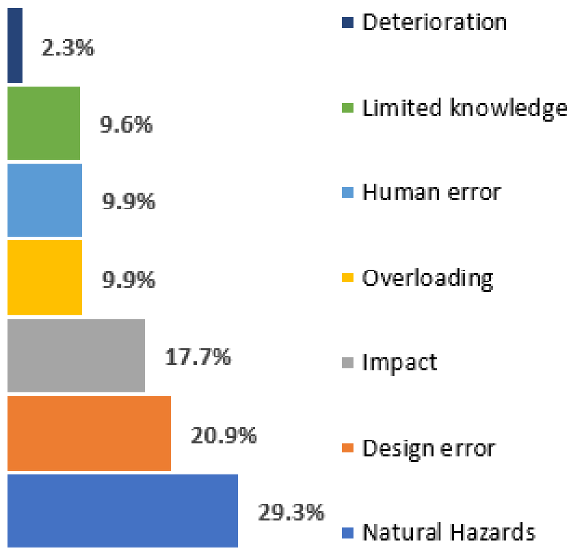

Figure 2. Collapse of bridges due to different reasons [27].

Experimental models were often employed for studying various problems [29-31]. For the scour issues around hydraulic structures, many studies were conducted. [32] used an experimental test to examine the 3D flow near a complex bridge pier, relations between its elements, and their impacts on flow. [33] studied the flow and scour around bridge piers with various formats and investigated for conditions with and without debris. [34] conducted laboratory analysis for the scour due to submerged vertical impinging circular jet. [35] conducted a laboratory study to examine the scour depth around bridge piers due to tsunamis. [36] examined the impact of pier nose extension on decreasing the scour depth using the experimental test at the laboratory. However, computational models are becoming better reliable and considered an excellent technique for modeling various engineering problems [37-43].

Moreover, the simulation approach of scouring has been enhanced due to the growing abilities of computational fluid dynamics (CFD) software, which is comparable to arranging an experiment. Therefore, the initial idea of this numerical simulation is to develop and create physical models that are difficult to set up in laboratory conditions by using numerical modeling [44]. One of the CFD software is FLOW 3D. It is computational fluid dynamics (CFD) software that can solve equations of multi-physics flow problems [45]. Besides, it includes numerical approaches to solve fluid movement equations and multi-scale multi-physics flow models. Users employ many fluid flows and heat transfer phenomena by integrating physical and numerical to solve different problems related to hydraulic engineering like scour [44]. Many studies were conducted to study the scour using FLOW 3D. [46] used FLOW 3D to assess its capability for imitating scour depth for non-cohesive sediment circumstances with different velocities. [47] used FLOW 3D to study the scour depth originated around the cylindrical pier under clear-water scour. [44] adopted FLOW 3D to model the debris effect on maximum scour hole depth at bridge piers.

[48] used FLOW 3D to investigate the impact of various turbulence flow pinnacles on the scouring pit of the bridge pier. [49] used the FLOW 3D model to demonstrate the performance of the software to imitate the flushing of reservoirs utilizing laboratory outcomes. [50] employed the FLOW 3D model to simulate and study the flow at the trapezoidal weir [51] used FLOW 3D to model and examine the scour around the submerged various slope angles sharp edge weir. [52, 53] used the FLOW 3D model to investigate the scour features of huge-diameter and multi-bucket bases in in-depth water locations.

As mentioned above, scour is a well-known factor that removes the river's bed material, and bridges collapse worldwide, especially during flood events. Therefore, the article aims to employ the CFD model using FLOW 3D to examine the scour around bridge piers and verify the efficiency of the FLOW 3D for modeling the scour around hydraulic structures like bridge piers.

2. Materials and Methods

2.1. Experimental Model

The experimental test was conducted at Hydraulic Laboratory at the University of Gaziantep by [54], it was performed using a rectangular flume (0.8m wide, 0.9m in length), and the diameter of the pier was 10 cm, which was placed at the center of the channel. The flow was 0.048 m^3/s, flow depth was 0.11 m, velocity was equal to 0.48 m/s, and bed material was non-cohesion sand with a median particle size d50 equal to 1.45 mm. Figure 3 shows the full details of the flume.

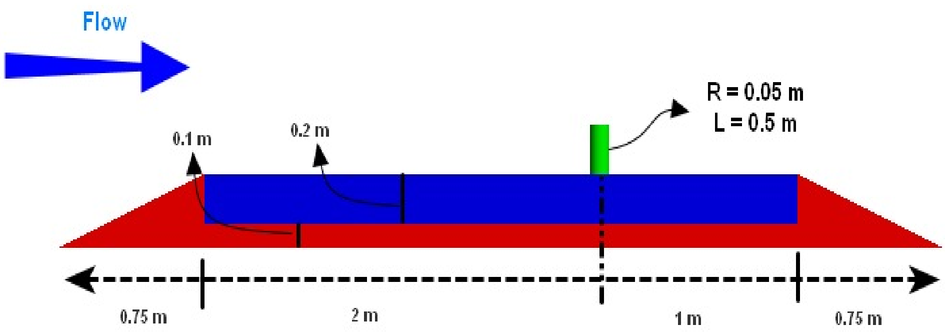

Figure 3. Layout of the flume.

2.2. FLOW-3D Model

In this investigation, the three-dimensional sediment scours model is designed to stimulate local scour around the bridge pier by utilizing FLOW 3D software. The system of the FLOW 3D is correctly coupled with fluid flow supports many non-cohesive species, deposition, bedload transport, and suspended load transport.

2.2.1. CFD Governing Equations of Scour Model

Elements of three-dimensional flow can manage run the scouring operation; the FLOW-3D Sediment Transport model can evaluate and analyze the scour and deposition process. The hydrodynamic simulation software is integrated with a sediment transport module with non-cohesive soil conditions that simulate bedload and suspended sediment transport, entrainment, and corrosion [55]. CFD equations of the scouring model were used to solve the sediment transportation as follows:

2.2.2. Bed Shear Stress

The shear stress is applied via the fluid on the packed bed surface, and defined as Eq. (1)

$$v = vt(\frac{1}{kc} \, ln \, ln \left(\frac{y}{\frac{vk}{ut}+ks}\right)) \tag{1}$$

vt shear velocity and $vt = \sqrt{\tau / \rho}$, τ bed shear stress, ρ is the bulk density of the fluid-sediment mixture, y is the distance from the wall, vk is the kinematic viscosity of the bulk flow, $kc = 0.4$ is the Von Karman fixe value, ks is the Nikuradse roughness. ks is linked to grain size as Eq. (2)

$$ks = csd_{50} \tag{2}$$

d_{50} grain diameter, cs is a factor equal to 2.5 as the recommended value.

2.2.3. Critical Shields Parameter

The Shields parameter is a dimensionless form of bed shear stress and defined as Eq. (3):

$$\theta sn = \frac{\tau}{g \; dn(\rho n - \rho f)} \tag{3}$$

where g is gravity, ρ_n is the mass density of sediment, d_n is grain diameter. The critical Shields parameter $\theta_{cs,n}$, as shown in Eq.(4), is used to define the critical bed shear stress τ_{csn}, at which sediment movement starts for both entrainment and bedload transportation,

$$\theta cs, n = \frac{\tau cs,n}{g \; dn(\rho n - \rho f)} \tag{4}$$

The primary worth of θ cs,n is for a flat and horizontal bed of identically-sized grains. Either determined by employees 0.05 by default or selected from the Soulsby-Whitehouse equation [56].

$$\theta cr, n = \frac{0.3}{1+1.2d,n} + 0.0055(-e^{-0.02d}) \tag{5}$$

2.2.4. Entrainment

The deposition and entrainment are dealt with as two dissent micro-processes synchronously. They are collective to control the net exchange rate among packed and suspended sediments, and entrainment. The velocity, at which the grains leave the packed bed, is the exciting velocity and is evaluated based on Winterwerp et al. [57], it is represented as Eq. (6):

$$(ulift, n = n_b a_n \, d_{*n}^{0.3} \; (Qn - Qcr, n)^{1.5} * \sqrt{gdn(sn-1)}) \tag{6}$$

2.3.5. Bedload Transport

The dimensionless formula of the bedload transference average for species n as Eq. (7)

$$\Phi n = (\frac{Qcb, n}{(g(sn-1)dn^3)^{.5}}) \tag{7}$$

where Q cs,n is the volumetric ability to transport the bed load average for each unit of bed width (in units of volume per width per time).Φn measured by applying the Meyer-Peter and Muller equation (1948), as shown in Eq. (8) [58].

$$\Phi n = Bn \, (\theta n - \theta cr, n)^{1.5} cb, n \tag{8}$$

where the coefficient of bedload is Bn, and it is commonly between (5.0, 5.7, 8.0, 13.0) respectively, for low, intermediate, and high sediment transportation

2.2.2. Modeling Steps

The CFD model was applied in Flow-3D by modeling a rectangular open channel with 0.8 m wide of the section work and a rectangular flume with a length of 2.5 m with two sold parts in the entrance of the flume and end of the flume with lengths 0.3 and 0.05, respectively. A vertical circular pier with a 0.05 m diameter and a 0.5 m height was used. The size of the sediment section was in the channel bed with 0.8 m width, 1.8 m length, 0.2m depth, and the full flume is 2.5 m with 0.5 m height and 0.8 m wide. Besides, two rigid elements were constructed in the outer sides of the geometry of both the channel's initial and final sections to prepare the water flow depth to start at the upper edge of the sediment to prevent disruption of the sediment bed section at the beginning of the simulation. The particle size diameter was 0.00145 m with a density of 2650 kg/m3 with a critical shields number of 0.05 and a drag coefficient of 0.5. A mesh block with 3097 cells was fitted to the model geometry, as shown in Figure 4. Besides, two mesh planes with more acceptable resolutions were defined around the pier in x and y directions to improve the model accuracy around the pier, shown in Figures 4, 5, and 6.
The mesh design is one of the most critical variables affecting models' accuracy, which depends on the volume and number of the cells and the intensified location of cells. Also, it might affect simulation duration.

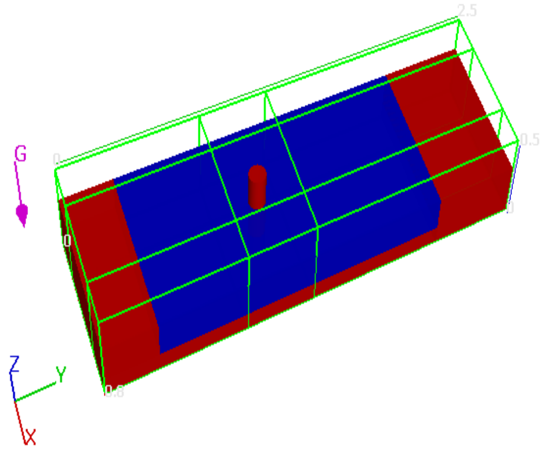

Figure 4. 3D meshing of plane around a cylindrical pier.

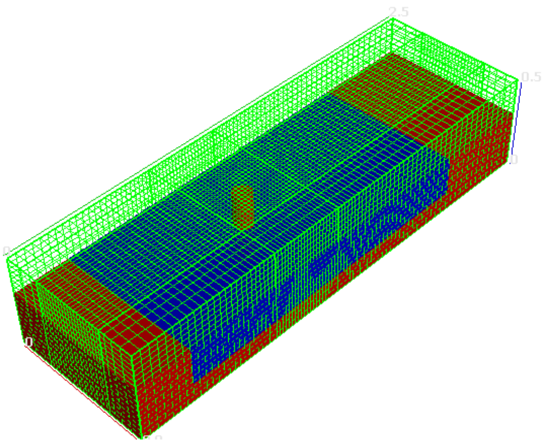

Figure 5. 3D meshing for the flume.

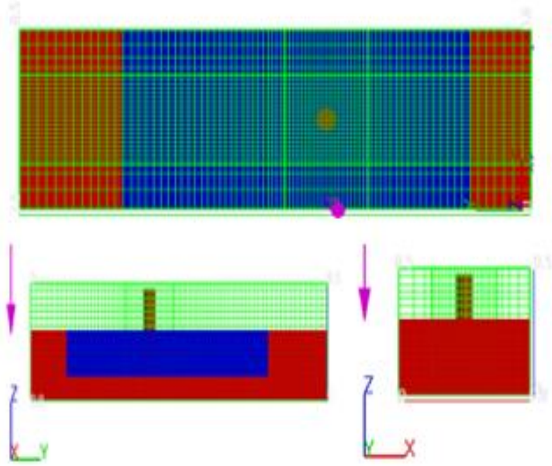

Figure 6. Various views of meshing.

Table 1 represents the size and number of meshes and the area of the intensity of the mesh in the two directions, X and Y. The intensification will be around the pier as a square plan; also, the pier is set in the middle of the square, as shown in Figure 4 from the top view.

Table 1 Mesh of FLOW-3D model

	Mesh size	
Mash block Length	Size of the cells	Number of the cells
0.4 * 04	0.03	38,097
0.4 * 0.4	0.025	64,000
0.4 * 0.4	0.02	125,000

2.2.2. Model Control and Boundary Conditions

Choosing proper boundary conditions for the hydraulic analysis is essential for numerical simulation. So, the numerical model should correspond to the physical needs of the problem. Therefore, to set up the numerical model, the boundary conditions and several crucial parameters should be conducted appropriately as they directly influence the results. The velocity in this study was assumed as live bed conditions depending on the experimental research.

Table 2. Modeling parameters

Details			
Mesh cell number	64,000	Sediment size (mm)	1.45
Turbulent model	Re-Normalized Group (RNG)	Density of sediment	2650(kg/m^3)
Water velocity	0.48 m/s	Pier diameter	50 mm
Water condition	Live bed scour	Channel width	0.8 m

As shown in Figure 7, the boundary conditions were specified. The discharge rate is selected for the inlet boundary in Y_{min}. Outflow at the outlet in Y_{max}, the water velocity in the inlet is 0.48 m/s. The depth of water is 11 cm. The inlet boundary has specified pressure and velocity depending on the modal conditions. The right and the left sides for X_{min} and X_{max} are considered a wall, Z_{min} in the bottom as the wall, and specified pressure on the top of the boundary Z_{max} to simulate open channel conditions. Figure 7 shows the model boundary conditions and geometry of the flume and plane meshing of the model for simulation of scour around a cylindrical pier.

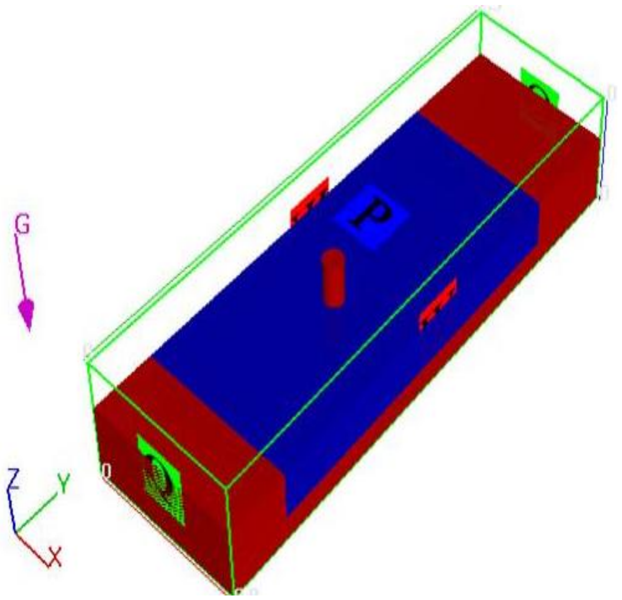

Figure 7. Boundary conditions of the numerical model.

3. Results and Discussion

The numerical simulation was performed in similar circumstances to the experimental model to examine the FLOW 3D model performance and study the velocity, and local scour depth around the bridge pier. Also, the influence of the scour on the bed elevation around a cylindrical bridge pier was analyzed by comparing the result with the experimental test. Figure 8 shows the regression value for experimental and numerical models.

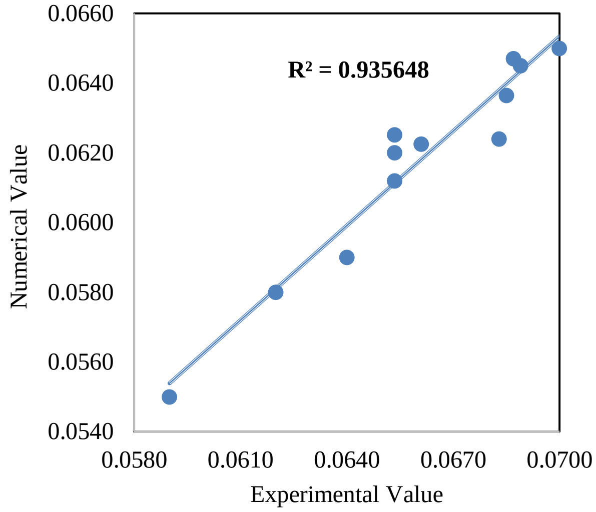

Figure 8 The calibration values of the test.

3.1. Flow and Velocity Around the Pier

The pier in the canal acts as an obstruction against the water. The flow was uniform around the specific velocity of 0.48 m/s until reaching the pier's location. Besides, it can be observed from Figure 9 that the velocity is higher when the water reaches both sides of the pier. The dark blue vectors in the opposite direction represent that flow reversion happens in the scour hole, as shown in Figure 10, creating a vortex that started at the bottom of the pier due to downward flow.

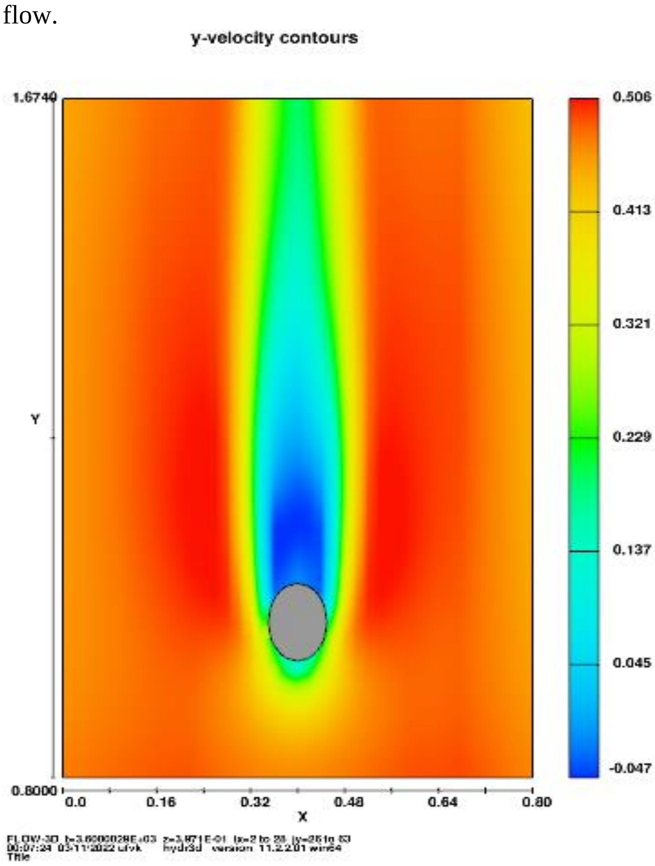

Figure 9. 2D average flow velocity.

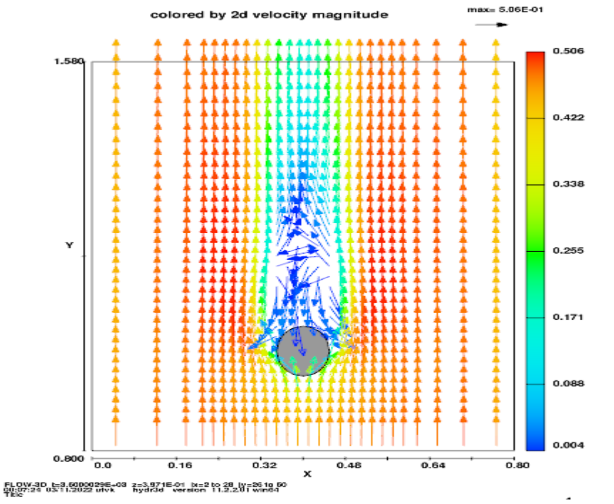

Figure 10. Vectors around the pier after halftime of the simulation run.

Also, the velocity gradually decreases as it approaches the canal's bed, as observed in Figure 10a-b at the front side of the pier gradually down and similarly rears the pier. This creates a difference in the pressure around the pier, generating a vortex where it becomes more intense on the front side of the pier. Also, Figure 11 cannot confirm by Compering the velocity in front and rear of the pier in both models with the advantage for the CFD to present more data.

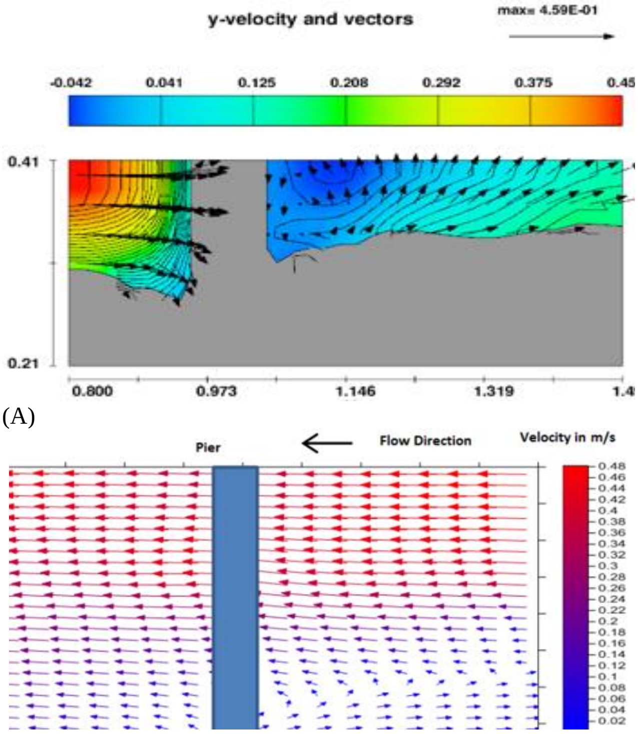

Figure 11. Compering the velocity in front and rear of the pier in both model (A) Numerical model pier (B) Circular pier (Adopted from [54]).

3.2. Simulated Scour Depth

In this CDF study, the simulated model in the Flow-3D result of the maximum scour depth was around 6.5 cm and 6.9 cm for the experimental model. The results indicated that the physical and numerical simulations were close to the maximum scour depth. With a slight difference in the formation of the erosion hole and the formation of sediments at the bed of the canal, as shown in the Figure12.

The maximum depth of scouring simulation appears to be on either side of the pier but slightly directly in front of the pier. Hence, the CFD outcomes give a somewhat lower assessment than the experimental model, as shown from the Longitudinal scour profile in Figure 13.

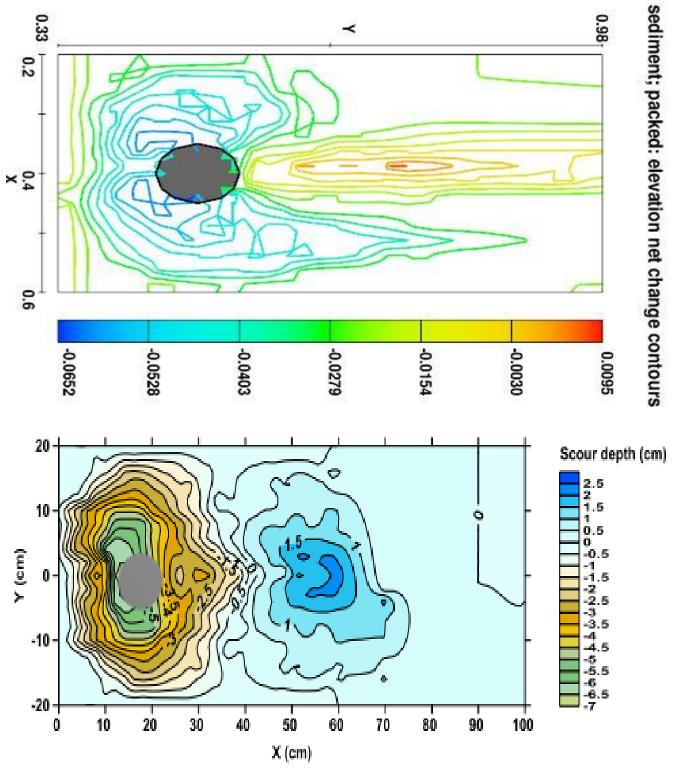

Figure 12. Compering the couture lines of the scour depth profile around bridge pier for CFD and experiment results (Adopted from [54]).

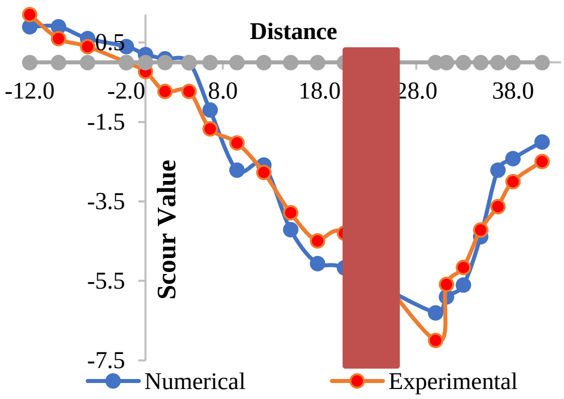

Figure 13. Longitudinal Scour profile

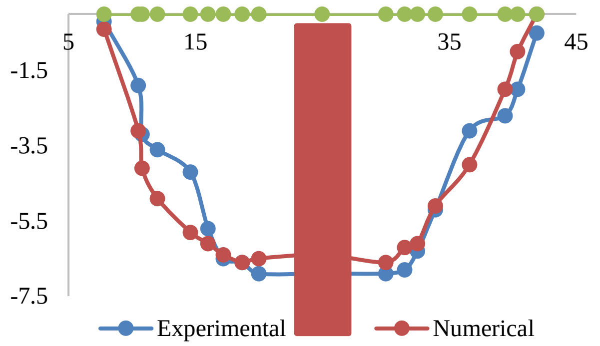

Figure 14. Transverse section scour profile

3.3. Development Scour Depth with Time

Figures 12 13and 14 show the transverse and longitudinal sections of the scour hole development around the bridge pier and changes in the elevations due to the canal's scour. The development of the maximum scour depth with time after one hour is illustrated in Figure 15 for the experimental and numerical model. The maximum scour depth for the FLOW-3D model was 6.5 cm and for the experimental was 6.9 cm. The results of the numerical model gave good agreement with the experimental. The numerical test stopped when the scour rate became around less than 5% of the pie diameter. At this point, we can determine the model reached the equilibrium stage.

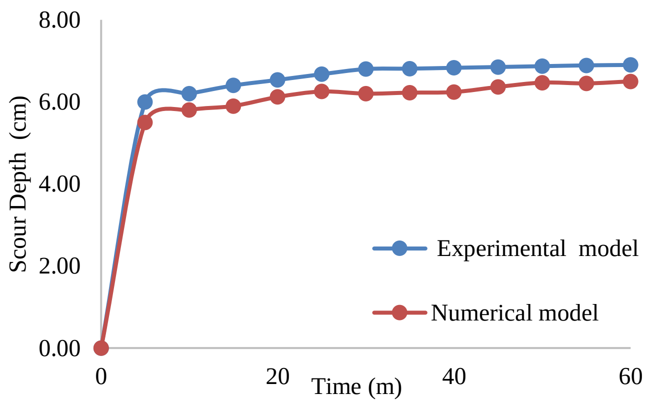

Figure 15. Development of the maximum scour depth with time.

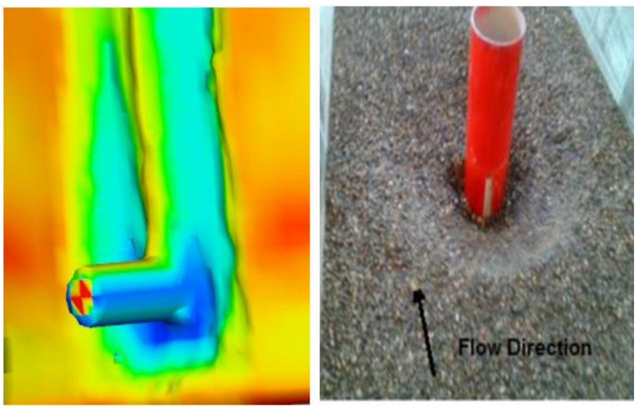

Figure 12. Experimental model and CFD channel bed formation after the full-time run (Adopted from [54]).

4. Conclusion

Bridge failure is often caused by scouring around bridge foundations in stream channels. Therefore, estimating the maximum scour depth is crucial for civil engineers. The current study uses the CFD model to simulate the scour phenomena by selecting a circular pier from an experimental study done by Ismael et al., 2015 and calibrated the model within the same conditions to control and ensure the accuracy of the results. Besides, the FLOW-3D model showed an error equal to 10% compared to the laboratory model. The primary outcomes of the study are as follows:

- These results show that the proposed numerical model Flow-3D is an efficient tool for simulating scour depth and flow around the bridge's pier.
- The mesh is one of the influence factors in the modeling development, and it can impact the model accuracy
- The Flow-3D running time can take up to three days and more in some cases.
- This study shows that Flow 3D can accurately evaluate the maximum scour depth.
- The numerical model results for the circular pier gave the lowest assessment of the scour depth at the front of the pier compared to the experimental outcomes in the same place.
- The model's ability to simulate the scour shape is dependent on the cross-section shape and flow properties.

For further development of this study, these suggestions can be considered:

- Increasing the number of cells and decreasing the size of the mesh can show more accurate results
- Examining the effect of parameters like sediment features, flow depth, flow velocity on the modeling
- Exploring the relation between the maximum scour depth and equilibrium scour.
- Modeling of scour depth around various shapes of bridge piers.
- Examining the performance of the FLOW-3D model with different experimental tests of scour around hydraulic structures.
- Artificial intelligence or machine learning can be used beside CFD model to predict and compare the local scour phenomena results for future research. Moreover, CFD modeling can be applied to study local scour and the counter measurement methods to reduce the scour depth around the bridge pier.

Conflict of Interest Statement

The authors declare no conflict of interest.

References

[1] K. Azizi, C.I. Meier, Urban Pluvial Flood Risk Assessment: Challenges and Opportunities for Improvement Using a Community-Based Approach, World Environmental and Water Resources Congress 2021, 350–361.

[2] K. Azizi, C.I. Meier, Improving the Characterization of Urban Flash Floods through Application of Local Knowledge, AGU Fall Meeting Abstracts, 2020, H162-0011.

[3] K. Azizi, C.I. Meier, L. Saija, Bottom-Up Planning: From Natural Disaster to Community Disaster, AGU Fall Meeting Abstracts, 2018, PA23F-1032.

[4] A. S. A. Ali, S. Ebrahimi, M. M. Ashiq, M. S. Alasta, B. Azari, CNN-Bi LSTM neural network for simulating groundwater level, Environ Eng, 8 (2022) 1–7.

[5] B. Azari, K. Hassan, J. Pierce, S. Ebrahimi, Evaluation of Machine Learning Methods Application in Temperature Prediction, Environmental Engineering 8 (2022) 1–12.

[6] S. Ebrahimi, M. Khorram, Variability effect of hydrological regime on river quality pattern and its uncertainties: case study of Zarjoob River in Iran, Journal of Hydroinformatics 23 (2021) 1146–1164.

[7] A.R. Kashani, C.V. Camp, M. Rostamian, K. Azizi, A.H. Gandomi, Population-based optimization in structural engineering: a review, Artif. Intell. Rev. 55 (2022) 345–452.

[8] A.R. Kashani, C.V. Camp, K. Azizi, M. Rostamian, Multi-objective optimization of mechanically stabilized earth retaining wall using evolutionary algorithms, Int J Numer Anal Methods Geomech 46 (2022) 1433–1465.

[9] M. Akhani, A.R. Kashani, M. Mousavi, A.H. Gandomi, A hybrid computational intelligence approach to predict spectral acceleration, Measurement: Journal of the International Measurement Confederation 138 (2019) 578–589.

[10] M. Gandomi, A.R. Kashani, A. Farhadi, M. Akhani, A.H. Gandomi, Spectral acceleration prediction using genetic programming based approaches, Appl. Soft Comput. 106(C) (2021) 13.

[11] A.R. Kashani, M. Akhani, C.V. Camp, A.H. Gandomi, A neural network to predict spectral acceleration, Basics of Computational Geophysics, Elsevier (2021) 335–349.

[12] B. Azari, M. Tabesh, Optimal design of stormwater collection networks considering hydraulic performance and BMPs, International Journal of Environmental Research 12 (2018) 585–596.

[13] B. Azari, M. Tabesh, Urban storm water drainage system optimization using a sustainability index and LID/BMPs, Sustainable Cities and Society 76 (2022) 103500.

[14] H. Breusers, G. Nicollet, H. Shen, Local scour around cylindrical piers, Journal of Hydraulic Research 15 (1977) 211–252.

[15] P. Khwairakpam, A. Mazumdar, Local scour around hydraulic structures, International Journal of Recent Trends in Engineering 1 (2009) 59.

[16] Shakir Ali Ali A, Günal M. Artificial Neural network for estimation of local scour depth around bridge piers. Archives of Hydro-Engineering and Environmental Mechanics 68 (2021).

[17] O. Link, C. Castillo, A. Pizarro, A. Rojas, B. Ettmer, C. Escauriaza, S. Manfreda, A model of bridge pier scour during flood waves, Journal of hydraulic research 55 (2017) 310–323.

[18] W.H. Hager, J. Unger, Bridge pier scour under flood waves, Journal of Hydraulic Engineering 136 (2010) 842–847.

[19] L.J. Prendergast, K. Gavin, A review of bridge scour monitoring techniques, Journal of Rock Mechanics and Geotechnical Engineering 6 (2014) 138–149.

[20] O. Link, S. Henríquez, B. Ettmer, Physical scale modelling of scour around bridge piers, Journal of Hydraulic Research 57 (2019) 227–237.

[21] B.W. Melville, A.J. Raudkivi, Flow characteristics in local scour at bridge piers, Journal of Hydraulic Research 15 (1977) 373–380.

[22] Y.M. Chiew, B.W. Melville, Local scour around bridge piers, Journal of Hydraulic Research 25 (1987) 15–26.

[23] H. Qi, W. Tian, H. Zhang, Modeling Local Scour around a Cylindrical Pier with Circular Collar with Tilt Angles (Counterclockwise around the Direction of the Channel Cross-Section) in Clear-Water, Water 13 (2021) 3281.

[24] B.W. Melville, S.E. Coleman, Bridge scour, Water Resources Publication, 2000.

[25] A. Parola, D. Hagerty, D. Mueller, B. Melville, G. Parker, J. Usher, The need for research on scour at bridge crossings, Stream Stability and Scour at Highway Bridges: Compendium of Stream Stability and Scour Papers Presented at Conferences Sponsored by the Water Resources Engineering (Hydraulics) Division of the American Society of Civil Engineers, ASCE, (1997) 1020–1020.

[26] A. Shirole, R. Holt, Planning for a comprehensive bridge safety assurance program, Transportation Research Record 1290 (1991) 290–005.

[27] D. Imhof, Risk assessment of existing bridge structures, university of cambridge, (2004).

[28] K. Wardhana, F.C. Hadipriono, Analysis of recent bridge failures in the United States, Journal of performance of constructed facilities 17 (2003) 144–150.

[29] A. Iqbal, H.S.U. Rehman, M. Munir, M. Ashiq, A. Omar, Z. Haider, M. Akhtar, M. Javed, O. U. U. Rehman, M. Adnan, M. Jahanzaib, Time and Cost Overrun in Construction Projects of Pakistan, Pakistan Journal of Engineering and Technology 2 (2019) 22–29.

[30] A. Iqbal, M. Yousuf, K. Ullah, M. Adnan, M. Ahmad, M. Ashiq, U. Shehzad, M. Munir, S. U. Rehman, M. Akhtar, M. Rizwan, M. Javed, U. Akram, Utilization of Waste Plastic Polymers to Improve the Performance of Modified Hot Mix Asphalt, Pakistan Journal of Engineering and Technology 3 (2020) 162–171.

[31] M. Jahanzaib, A. Iqbal, H. Ashfaq, M. Munir, M. Akhtar, M. Ashiq, B. Ibrahim, Partial Replacement of Coarse Aggregate by Using Pumice Aggregate in Lightweight Concrete-Experimental Investigation, Pakistan Journal of Engineering and Technology 4 (2021) 27–30.

[32] A. Beheshti, B. Ataie-Ashtiani, Experimental study of three-dimensional flow field around a complex bridge pier, Journal of engineering mechanics 136 (2010) 143–154.

[33] E. Rahimi, K. Qaderi, M. Rahimpour, M.M. Ahmadi, Effect of debris on piers group scour: An experimental study, KSCE Journal of Civil Engineering 22 (2018) 1496–1505.

[34] R. Shakya, V. Sarda, M. Singh, Experimental Study on Scour Due to Submerged Vertical Impinging Circular Jet, Transportation, Water and Environmental Geotechnics, Springer (2021) 337–345.

[35] O. Suaznabar, N. Sinha, M.A. Sitek, S. Lottes, N. Zhang, Pier Scour Estimation for Tsunami at Bridges [techbrief], United States. Federal Highway Administration. Office of Research …, 2021.

[36] J.A. Sharp, T.O. McAlpin, Case Study: Experimental Investigation into the Feasibility of Pier Nose Extensions to Reduce Local Scour around Bridge Piers, Journal of Hydraulic Engineering 148 (2022) 05021010.

[37] M. Nikian, M. Naghashzadegan, Modeling of Solar Radiation on Part Shaded Walls, SIMS 2004 (2004) 173.

[38] M. Naeej, M. Naeej, J. Salehi, R. Rahimi, Modeling and Evaluating of Wave Run-up and Overtopping using Smoothed Particle Hydrodynamics Method, Computational Research Progress in Applied Science and Engineering 3 (2017) 25–34.

[39] M. M. Ashiq, H. ur Rehman, N. M. Khan, Impact of large diameter recharge wells for reducing groundwater depletion rates in an urban area of Lahore, Pakistan, Environmental Earth Sciences 79 (2020) 1–14.

[40] G. Tunc, M.M. Othman, H.C. Mertol, Finite Element Analysis of Frames with Reinforced Concrete Encased Steel Composite Columns, Buildings 12(3) (2022) 375.

[41] S. Sun, M. Zhou, W. Lu, A. Davarpanah, Application of symmetry law in numerical modeling of hydraulic fracturing by finite element method, Symmetry 12(7) (2020) 1122.

[42] G.J. Houben, L. Stoeckl, K.E. Mariner, A.S. Choudhury, The influence of heterogeneity on coastal groundwater flow-physical and numerical modeling of fringing reefs, dykes and structured conductivity fields, Advances in Water Resources 113 (2018) 155–166.

[43] M.M. Hamed, A. Al-Masri, Z.M. Dalala, R.J. AlSaleh, Modeling the Time Duration Until the Adoption of Residential Rooftop Solar Photovoltaic Systems, Journal of Energy Resources Technology 144 (2021).

[44] H.K. Jalal, W.H. Hassan, Three-dimensional numerical simulation of local scour around circular bridge pier using Flow-3D software, IOP Conference Series: Materials Science and Engineering, IOP Publishing (2020) 012150.

[45] M. Nazari-Sharabian, A. Nazari-Sharabian, M. Karakouzian, M. Karami, Sacrificial piles as scour countermeasures in river bridges a numerical study using flow-3D, Civil Engineering Journal 6 (2020) 1091.

[46] M. Ghasemi, S. Soltani-Gerdefaramarzi, The scour bridge simulation around a cylindrical pier using Flow-3D, Journal of Hydrosciences and Environment 1 (2017) 46–54.

[47] I.S.P. Mendonça, H.D.L. Canilho, C.M.S. Fael, Flow-3D Modelling of the Debris Effect on Maximum Scour Hole Depth at Bridge Piers, 38th IAHR World Congress (2019) 2813–2821.

[48] C. Man, G. Zhang, V. Hong, S. Zhou, Y. Feng, Assessment of turbulence models on bridge-pier scour using Flow-3D, World Journal of Engineering and Technology 7 (2019) 241–255.

[49] M. Sadat Helbar, A. Parvaresh Rizi, J. Farhoudi, A. Mohammadi, 3D flow simulation to improve the design and operation of the dam bottom outlets, Arabian Journal of Geosciences 14 (2021) 1–11.

[50] O. Setyandito, S. Christian, R. Lopa, Flow Characteristics Investigation On Trapezoidal Weir Using FLOW 3D, IOP Conference Series: Earth and Environmental Science, IOP Publishing (2022) 012013.

[51] M. Rostam Abadi, S. Kazemi Mohsenabadi, Numerical study of the weir angle on the flow pattern and scour around the submerged weirs, International Journal of Modern Physics C (2022) 2250110.

[52] J. Lian, J. Li, Y. Guo, H. Wang, X. Yang, Numerical study on local scour characteristics of multi-bucket jacket foundation considering exposed height, Applied Ocean Research 121 (2022) 103092.

[53] S. Khani, M.A. Moghadam, M. Nikookar, Pressure Fluctuations Investigation on the Curve of Flip Buckets Using Analytical and Numerical Methods, Computational Research Progress in Applied Science & Engineering 03 (2017)165–171.

[54] A. Ismael, M. Gunal, H. Hussein, Effect of Bridge Pier Position on Scour Reduction According to Flow Direction, Arabian Journal for Science and Engineering 40 (2015) 1579–1590.

[55] X. Lu, X. Wang, X. Ban, V.P. Singh, Transport characteristics of non-cohesive sediment with different hydrological durations and sediment transport formulas, Journal of Hydrology 591 (2020) 125489.

[56] R. Soulsby, R. Whitehouse, Threshold of Sediment Motion in Coastal Environments, In: Pacific Coasts and Ports '97: Proceedings of the 13th Australasian Coastal and Ocean Engineering Conference and the 6th Australasian Port and Harbour Conference; Volume 1. Christchurch, N.Z.: Centre for Advanced Engineering, University of Canterbury, (1997) 145–150.

[57] J.C. Winterwerp, W.T. Bakker, D.R. Mastbergen, H.v. Rossum, Hyperconcentrated Sand‐ Water Mixture Flows over Erodible Bed, Journal of Hydraulic Engineering 118 (1992) 1508–1525.

[58] E. Meyer-Peter, R. Müller, Formulas for bed-load transport, IAHSR 2nd meeting, Stockholm, appendix 2, IAHR, 1948.